

Surface Creasing Instability of Soft Polyacrylamide Cell Culture Substrates

Krishanu Saha,[†] Jungwook Kim,[¶] Elizabeth Irwin,[‡] Jinhwan Yoon,[†] Farhana Momin,[¶] Verónica Trujillo,[¶] David V. Schaffer,^{†‡} Kevin E. Healy,^{‡§} and Ryan C. Hayward^{¶*}

[†]Department of Chemical Engineering, [‡]Department of Bioengineering, and [§]Department of Materials Science and Engineering, University of California, Berkeley, California; and [¶]Department of Polymer Science and Engineering, University of Massachusetts, Amherst, Massachusetts

ABSTRACT Efforts to understand and engineer cell behavior in mechanically soft environments frequently employ two-dimensional cell culture substrates consisting of thin hydrogel layers with low elastic modulus supported on rigid substrates to facilitate culturing, imaging, and analysis. Here we characterize how an elastic creasing instability of the gel surface may occur for the most widely used soft cell culture substrate, polyacrylamide hydrogels, and show that stem cells respond to and change their behavior due to these surface features. The regions of stability and corresponding achievable ranges of modulus are elucidated in terms of the monomer and cross-linker concentrations, providing guidance for the synthesis of both smooth and creased soft cell substrates for basic and applied cell engineering efforts.

Received for publication 20 July 2010 and in final form 20 September 2010.

*Correspondence: rhayward@mail.pse.umass.edu

The mechanical properties of the substrate or matrix play a critical role in cell motility, cytoskeletal organization, gene expression, and stem cell differentiation (1–5). Designing materials for in vitro cell culture and tissue engineering applications therefore requires careful attention to both mechanical and biochemical properties. The model material system most commonly employed for studies of substrate stiffness effects is covalently cross-linked hydrogels of polyacrylamide (pAAM), which can be formulated with moduli covering a wide range of physiologically relevant values, ~0.010–50 kPa (5). Thin layers (~10–500 μm) are typically used, yielding flexible and often fragile gels that are coated on a rigid substrate, e.g., a glass coverslip, to facilitate handling.

A commonly encountered, but poorly characterized, problem arises when the modulus of the gels is reduced too far: sharp lines resembling cracks may appear on the surface of the gel upon immersion in aqueous media (2,6–8). These features result from attachment of the gel to a rigid substrate. When the gel is immersed in an aqueous environment, it swells due to the osmotic pressure difference with the surrounding medium, and equilibrium is attained when this osmotic pressure difference is matched by the elastic stress required to expand the cross-linked polymer network. An unconstrained gel swells in all dimensions, but a thin layer on a rigid substrate can only expand in the normal direction due to its anchoring to the surface. This produces an equibiaxial compressive stress within the film, which can induce buckling of the surface into sharp folds, or creases, with a characteristic spacing proportional to the film thickness.

A typical creased pAAM gel surface exhibits a series of sharp lines with occasional branching points (Fig. 1 A). To verify that these are folds, we fluorescently stained the near-surface region before onset of the instability (see the [Supporting Material](#)), then subsequently swelled the gel in water. As shown by confocal fluorescence microscopy (Fig. 1 B), the sharp features correspond to zones of subduc-

tion of the free surface into the gel layer below, rather than gaps in fluorescence, as expected for cracks.

The topography formed due to creasing may significantly influence cell behavior (2,8,9), thus it is critical that this instability be understood and controlled. To demonstrate the relevance of surface creases to in vitro cell behavior, adult neural stem cells were cultured on pAAM surfaces grafted with laminin or bsp-RGD(15) peptide (2). Cells on flat surfaces uniformly attached and differentiated (Fig. 2, right), whereas cells on creased surfaces migrated to folds and adopted mature lineage-committed neuronal and astrocytic phenotypes (Fig. 2, left). Clear alignment of neurites from neurons occurred on the creased pAAM gel (Fig. 2 B, left).

The onset of creasing can be characterized in terms of the effective compressive strain experienced by the surface-attached gel. If an unconstrained gel swells by a factor λ_f in each dimension, then the effective strain ε experienced by an identical gel grafted to a rigid substrate is defined by $\varepsilon = 1 - \lambda_f^{-1}$. Our previous study of pAAM gels, with estimated shear moduli G of ~0.6–24 kPa and thicknesses of 3 μm –1 mm, yielded creases beyond a critical strain ε_c ranging from 0.30 to 0.37 with an average of 0.33 (7). The insensitivity of ε_c to material properties and length scale agrees with theoretical predictions (11), and suggests that the key to preventing creases is to tune the balance between modulus and osmotic stress to maintain a level of swelling below $\lambda_f \approx 1.5$. We first consider how these two factors depend on gel composition, then validate this approach using the model system of pAAM gels containing varying contents of AAM monomer w_m and bisacrylamide (Bis) cross-linker w_x (Table 1).

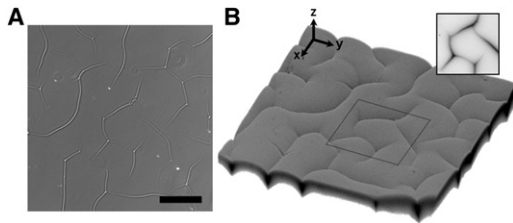


FIGURE 1 (A) Phase-contrast optical image of a creased pAAm gel surface (1 kPa; 10 wt % AAm, 0.01 wt % sodium acrylate, 0.02 wt % Bis. Scale bar, 200 μm). (B) A confocal fluorescence image (x,y,z scale 1:1:3) after swelling reveals sharp folds in the gel surface (*inset*: x - y slice 32 μm below the surface).

According to classical theories of network elasticity, the shear modulus is proportional to the density of elastically active strands times thermal energy $k_B T$. For the affine model (12) of a network with N Kuhn steps of length b between junctions, and polymer volume fraction ϕ_0 ,

$$G = \frac{\phi_0}{b^3 N} k_B T. \quad (1)$$

Thus, the modulus scales linearly with the concentration of polymer in the gel, but inversely with the length of the chains. In the idealized case that each cross-linker is active and every monomer is incorporated into the network, N is proportional to the ratio of monomer to cross-linker concentrations. Because ϕ_0 is also proportional to monomer concentration (assuming the amount of cross-linker is small), we may expect from Eq. 1 that G should be proportional to w_x and independent of w_m . In reality, nonidealities in gel structure generally make G an increasing function of both monomer and cross-linker concentration.

The osmotic stress π driving swelling of a polymer gel is roughly equal to that of a semidilute polymer solution of the same composition. When immersed in a good solvent, the initial driving force for swelling (12) is given by

TABLE 1 Compositions and moduli of pAAm gels

AAm* content w_m (wt %)	Bis† content w_x (wt %)	G' (Pa)
3.0%	0.02–0.2%	12–160
5.0%	0.02–0.2%	60–1100
7.5%	0.02–0.2%	—
10.0%	0.02–0.2%	400–9600
12.0%	0.02–0.2%	—

*Acrylamide.

†Bisacrylamide.

$$\pi \sim \frac{\phi_0^{2.3}}{b^3} k_B T. \quad (2)$$

This is a strongly-increasing function of polymer concentration, but does not depend on N , thus it is nearly independent of cross-linker concentration. Because swelling is determined by a balance between G and π , comparing Eq. 1 and Eq. 2 suggests that λ_f can be reduced while maintaining fixed G by decreasing ϕ_0 (or w_m) and simultaneously increasing w_x .

To test this assertion, we studied pAAm gels where at each composition (Table 1) two identical gels were polymerized between coverslips; however, in one case the bottom coverslip was treated with an adhesion promoter, whereas in the other case it was treated with a release coating allowing unconstrained swelling. Equilibrium values of λ_f for unconstrained gels are plotted in Fig. 3 A, with open symbols representing compositions where surface-attached gels formed creases and solid symbols representing those that did not.

Two important points should be noted. First, whereas λ_f increases as w_x is lowered for all values of w_m , there is no simple trend in the dependence of swelling on w_m . This is at first surprising, because the prediction for a covalently cross-linked network swelled in a good solvent (13) is

$$\lambda_f \sim \phi_0^{0.25} N^{0.2}, \quad (3)$$

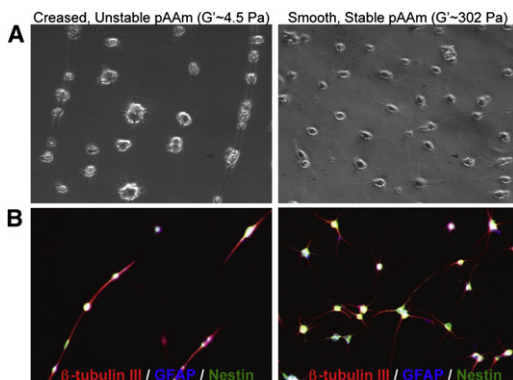


FIGURE 2 (A) Phase-contrast images indicate that adult neural stem cells sensed the surface creases and projected neurites along the creases on the unstable pAAm formulation. (B) Immunostaining for cell phenotypes (10).

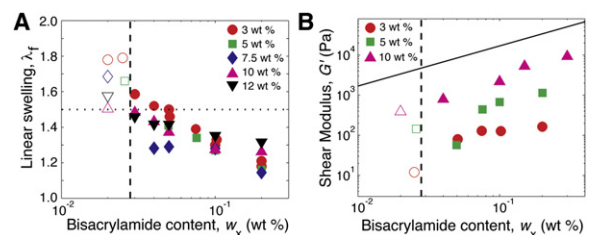


FIGURE 3 (A) Linear swelling λ_f versus Bis content w_x for different AAm contents w_m (see *legend*). Open symbols represent compositions where surface-attached gels formed creases. Dotted and dashed lines at $\lambda_f = 1.5$ and $w_x = 0.028$ wt %, respectively, delineate creased from stable gels. (B) Shear moduli G' of pAAm gels. (*Open symbols*) Compositions where surface-attached gels formed creases. (*Solid line*) Predicted modulus if all cross-links were elastically active. Estimated uncertainties correspond approximately to marker sizes in both plots.

and raising w_m at fixed w_x should increase both ϕ_0 and N . However, nonidealities in network structure can again lead to significant deviations from this prediction, and prior reports have even shown nonmonotonic dependence of swelling on monomer concentration for similar systems (14). The second point concerns the transition from the flat to the creased state for surface-attached gels. The dotted line at $\lambda_f = 1.5$, corresponding to the previously-established criterion of $\varepsilon_c \approx 0.33$ (7), captures the onset of creasing with the exception of 3 wt % AAm gels (red circles in Fig. 3 A) where the transition occurs above $\lambda_f = 1.6$. Because swelling is largely insensitive to w_m , the transition from flat to creased states may also be described by the dashed line at $w_x = 0.028$ wt %, which cleanly divides the data over the full range of w_m studied. The guideline $\lambda_f \approx 1.5$ remains useful, because it is general to other chemistries and can thus be easily translated to different material systems.

The values of G' measured by oscillatory shear rheology (which are nearly equal to G for a predominantly elastic material) for gels with 3, 5, and 10 wt % AAm, plotted in Fig. 3 B (full data in Table S1 in the Supporting Material), are in good agreement with a previous study (5). The dashed line at $w_x = 0.028$ wt % again demarcates the transition from flat to creased supported gel samples. The solid line represents the predicted shear modulus if every cross-linker were elastically active: although the data follow the same trend, they fall below the predicted curve, also in agreement with the earlier study (5). Unlike the swelling data in Fig. 3 A, the modulus is quite sensitive to monomer concentration. For 10 wt % AAm, the modulus can be reduced to ~ 600 Pa by lowering Bis concentration, beyond which further reductions in w_x lead to creasing. By lowering the AAm concentration to 3 wt %, however, the modulus can be reduced below 100 Pa without triggering the surface instability. We have not studied the rheological properties of 12 wt % gels, but their moduli should be tunable from ~ 50 kPa at high cross-linker concentration down to ~ 2 kPa before the onset of creases (5). Thus, appropriate choices of monomer and cross-linker content allow the modulus to be tuned from 50 kPa to below 100 Pa without encountering creases.

We offer one caveat: even if the composition is chosen to avoid creases, substantial swelling of the surface-attached gel (up to ~ 2 -fold) (7) may occur. Thus, the modulus of the swelled gel will be slightly different than determined by rheology for the unswelled gel, and in general, there may be significant anisotropy between the in-plane and out-of-plane incremental moduli due to the lateral prestress in the swollen surface-attached gel. For gels close to the instability, traction forces applied by the cell may even exceed the critical compression and cause local folding. Rather than managing the balance between osmotic stress and gel modulus, an alternative approach that avoids these complications is to eliminate swelling stresses altogether by allowing an unconstrained gel to swell freely and subsequently attach-

ing it to a rigid support. Although we have found this method to be effective for preparing gels with moduli of ~ 0.5 kPa and above, it is difficult especially for soft gels and likely not suitable for high-throughput cell-based studies.

In summary, surface creasing of pAAm substrates can significantly influence cell behavior and must be carefully considered for the soft substrates increasingly used in mechanotransduction experiments. We anticipate that this work can guide the synthesis of both smooth and creased soft cell substrates for cell engineering efforts.

SUPPORTING MATERIAL

Materials and methods, complete modulus and swelling data for Fig. 3B, and references are available at [http://www.biophysj.org/biophysj/supplemental/S0006-3495\(10\)01195-1](http://www.biophysj.org/biophysj/supplemental/S0006-3495(10)01195-1).

ACKNOWLEDGMENTS

This work was supported by National Institutes of Health grant No. R21DE18044 and National Science Foundation grant No. DMR-0747756. K.S. is supported by a Society in Science: Branco-Weiss fellowship.

REFERENCES and FOOTNOTES

- Engler, A. J., S. Sen, ..., D. E. Discher. 2006. Matrix elasticity directs stem cell lineage specification. *Cell*. 126:677–689.
- Saha, K., A. J. Keung, ..., K. E. Healy. 2008. Substrate modulus directs neural stem cell behavior. *Biophys. J.* 95:4426–4438.
- Discher, D. E., D. J. Mooney, and P. W. Zandstra. 2009. Growth factors, matrices, and forces combine and control stem cells. *Science*. 324:1673–1677.
- Isenberg, B. C., P. A. Dimilla, ..., J. Y. Wong. 2009. Vascular smooth muscle cell durotaxis depends on substrate stiffness gradient strength. *Biophys. J.* 97:1313–1322.
- Yeung, T., P. C. Georges, ..., P. A. Janmey. 2005. Effects of substrate stiffness on cell morphology, cytoskeletal structure, and adhesion. *Cell Motil. Cytoskeleton*. 60:24–34.
- Tanaka, T., S. Sun, ..., T. Amiya. 1987. Mechanical instability of gels at the phase transition. *Nature*. 325:796–797.
- Trujillo, V., J. Kim, and R. C. Hayward. 2008. Creasing instability of surface-attached hydrogels. *Soft Matter*. 4:564–569.
- Moshayedi, P., L. F. Costa, ..., K. Franze. 2010. Mechanosensitivity of astrocytes on optimized polyacrylamide gels analyzed by quantitative morphometry. *J. Phys. Condens. Matter*. 22:194114.
- Guvendiren, M., and J. A. Burdick. 2010. The control of stem cell morphology and differentiation by hydrogel surface wrinkles. *Biomaterials*. 31:6511–6518.
- Neuronal differentiation conditions (retinoic acid and forskolin) were used during culture. β -Tubulin III (red), GFAP (blue), and Nestin (green) mark neurons, astrocytes, and immature stem cells, respectively.
- Biot, M. 1963. Surface instability of rubber in compression. *Appl. Sci. Res.* 12:168–182.
- Rubinstein, M., and R. H. Colby. 2003. *Polymer Physics*. Oxford University Press, New York.
- Obukhov, S. P., M. Rubinstein, and R. H. Colby. 1994. Network modulus and superelasticity. *Macromolecules*. 27:3191–3198.
- Orakdogan, N., and O. Okay. 2006. Effect of initial monomer concentration on the equilibrium swelling and elasticity of hydrogels. *Eur. Polym. J.* 42:955–960.